THE ASTROPHYSICAL JOURNAL, 349:429–436, 1990 February 1

Lyα CLOUDS: ISOLATED STRUCTURES IN COLD DARK MATTER COSMOGONY?

ARIF BABUL
Princeton University Observatory
Received 1989 May 5; accepted 1989 July 20

ABSTRACT

Formation of low-mass objects is inevitable in a cold dark matter (CDM) cosmogony. Objects that exist in near-mean background density environments are most likely to survive destruction. Such objects will also not exhibit strong clustering. Models have been proposed seeking to identify these isolated low-mass condensates as Lyα cloud candidates. However, the accompanying estimates of quantities such as the epoch of formation, the number density of candidate objects, etc., are not based on characteristics of isolated density peaks. Isolated density peaks result primarily from power in a narrow band at the mass scale of the structures. In this paper, we introduce a filter designed to study isolated density fluctuations. We use the filter to identify Lyα cloud candidates in a biased CDM model. We find that the number density of cloud candidates at $z = 2.5$ is too small to account for the observed number of lines. If Lyα clouds have their origins in primordial density fluctuations, the CDM power spectrum does not have sufficient power on subgalactic scales to account for the observed structures.

Subject headings: cosmology — dark matter — galaxies: intergalactic medium — quasars

I. INTRODUCTION

There is a general agreement that the forest of lines, seen in absorption in the quasar spectra blueward of the Lyα emission, represents highly ionized intergalactic absorbing clouds (Sargent *et al.* 1980). High-resolution spectral observations show directly that these lines are distinct entities, "clouds," with the filling factor along any given line of sight of $f_c \lesssim 10^{-2}$ (Ostriker 1987). The Lyα clouds are thought to be photoionized by the intergalactic flux from quasars and galaxies, with the resulting gas temperature of $T \sim 3 \times 10^4$ K for a mean intensity of ionizing flux at Lyman limit of $J_\nu \sim 10^{-21}$ ergs cm^{-2} s^{-1} Hz^{-1} (Ikeuchi and Ostriker 1986). Equilibrium between ionization and recombination rates based on the above model suggests that the neutral fraction in the clouds is $n_{\rm H\,I}/n_{\rm H\,II} \approx 10^{-4}$. Foltz *et al.* (1984) inferred the cloud sizes to be $\sim$5–25 kpc from the detection of some but not all of the lines in the two images of the gravitationally lensed quasar 2345+007. With the cloud size known, the neutral hydrogen density and, therefore, the total gas density in the clouds can be estimated from the measured H I column density. The combination of the total gas density and the cloud sizes allows the baryonic mass of the clouds to be determined. The mass range for Lyα clouds is 10^7–$10^9\ M_\odot$.

A study by Steidel and Sargent (1987) of the Lyα forest and the Gunn-Peterson (GP) effect (Gunn and Peterson 1965) suggests that the Lyα clouds are high contrast entities with respect to the intercloud medium. The high-resolution statistical study of the Lyα forest revealed that the neutral hydrogen in the intercloud medium $n^M_{\rm H\,I}$ contributes $\lesssim$10% to the integrated Lyα absorption optical depth, as compared to the smoothed out neutral hydrogen density in the clouds. The latter can be expressed to $f_c \times n^c_{\rm H\,I}$ where $n^c_{\rm H\,I}$ is the neutral hydrogen number density in clouds; therefore,

$$\frac{n^c_{\rm H\,I}}{n^M_{\rm H\,I}} \gtrsim 10^3 \left(\frac{f_c}{10^{-2}}\right)^{-1} . \qquad (1)$$

The clouds must have been produced by a process which compressed preexisting gas by a significant amount.

Lyα clouds have been observed in the redshift interval $1.5 < z < 4.1$. The observed distribution in redshift of the Lyα lines along a given line of sight, with H I column densities 10^{14} cm^{-2} $< N_{\rm H\,I} < 10^{16}$ cm^{-2} and the rest-frame equivalent width greater than $W_c = 0.36$ Å (Bajtlik, Duncan, and Ostriker 1988 and references therein) is

$$\frac{dN_{\rm obs}}{dz} \approx 3(1+z)^{2.4} ; \qquad (2)$$

there are approximately 60 observed lines per unit redshift at $z \approx 2.5$. The average comoving distance between adjacent Lyα clouds along a line of sight in an $\Omega = 1$ universe is

$$\bar{R}(z) \equiv \frac{c}{H(z)}\left[\frac{dN_{\rm obs}}{dz}\right]^{-1} = 7.5 h_0^{-1}\left(\frac{1+z}{3.5}\right)^{-3.9} \text{ Mpc} , \qquad (3)$$

where h_0 is the current value of the Hubble's constant in units of 100 km s^{-1} Mpc^{-1}. Since the characteristic comoving scale for the local large-scale structure is $10 h_0^{-1}$ Mpc $< R < 30 h_0^{-1}$ Mpc (Huchra *et al.* 1987; Ostriker and Strassler 1989), the Lyα clouds at $z \gtrsim 2.5$ can be used to probe the arrangement of matter on these scales. Using the Lyα forest in this manner was first suggested by Oort (1981).

Most of the empirical studies of the Lyα cloud distribution have involved determining the two-point correlation function of absorption lines along lines of sight. Sargent *et al.* (1980) have shown the Lyα clouds exhibit no significant clustering on scales from $\sim$300 to 30,000 km s^{-1}. Recent evidence, though, suggests that the clouds cluster very weakly on scales $\sim$400 km s^{-1} and smaller (Webb 1987; Ostriker, Bajtlik, and Duncan 1988). Regardless, the distribution of Lyα clouds at $z \gtrsim 2.5$ is much more uniform than the present-day distribution of galaxies.

A possible explanation for the formation of the Lyα clouds can be found within the context of a biased cold dark matter (CDM) model. According to this hypothesis, galaxies and clusters are assembled through hierarchical clustering of lower mass condensates and correspond to large density peaks. An inevitable feature of such a model is the formation of low-mass objects $M \sim 10^7$–$10^{10}\ M_\odot$.

Rees (1986) proposed that the Lyα forest may be evidence for photoionized gas stably confined by the gravitational field of the dark matter minihalos. If the density within the minihalos is almost constant, the stability requirement is $C_s \lesssim V_g \lesssim \Omega_b^{-1/3} C_s$, where C_s is the sound speed in the gas and V_g is the virial velocity of the gas in the paraboloidal potential well. For an isothermal gas cloud at $T \approx 3 \times 10^4$ K, the above condition implies that 16 km s$^{-1} \lesssim V_g \lesssim 34$ km s^{-1}, assuming $\Omega_b \approx 0.1$.

Studying the confinement of $\sim 10^4$ K gas in subgalactic density peaks in greater detail led Bond, Szalay, and Silk (1988, hereafter BSS) to propose a dynamical model for the Lyα clouds; BSS investigated the baryon motions in collapsing density peaks subsequent to heating by photoionization at $z \approx 4$. They noted that depending on the height of the peak and its mass scale, the gas trapped in a collapsing CDM fluctuation either expands after photoionization or continues to collapse unaffected. The gas in density peaks of mass scales appropriate for Lyα cloud candidates generally undergoes expansion.

In a biased CDM scenario, the clustering of small-scale peaks arises due to statistical and dynamical effects (Bardeen *et al.* 1986, hereafter BBKS). Statistical clustering refers to the enhancement of the local number density of collapsing low-mass objects over the mean number density in regions where the local background mass density is higher than the mean. In the case of $\sim 10^9 M_\odot$ condensates, the statistical enhancement alone suggests that these objects ought to exhibit significant clustering tendencies; in regions destined to become bright galaxies, the number density of the subgalactic density peaks ought to exceed the mean number density by a factor of ~ 20 (BSS). To avoid strong statistical clustering, both Rees (1986) and BSS have stressed that the low-mass condensates in high-density environments would be destroyed by mergers accompanying the collapse of larger mass objects; furthermore, the formation of larger objects may generate environmental conditions that lead to expulsion of gas from the low-mass condensates. The surviving condensates are most likely to be in environments where the background mass density is not significantly different from the mean. These isolated low-mass density peaks would appear more uniformly distributed than the larger mass, high-density peaks that are identified as galaxies. Even "isolated" low-mass objects are subject to gravitational interactions, giving rise to dynamical clustering. Depending on the magnitude of this effect, it may serve to explain the very weak clustering observed in the Lyα cloud distribution.

In studying the formation of low-mass objects in a near-mean background environment, we are interested in identifying their epoch formation and we would like to calculate their number density. In the standard analysis of the CDM cosmogony, the epoch at which the bulk of structure of mass scale M enters the nonlinear collapse phase is estimated on the basis of threshold criterion, $\sigma_0(M) \sim 1$; $\sigma_0(M)$ is the rms fluctuation of the density field smoothed on mass scale M. The popular choices for the smoothing function are the Gaussian and the "top-hat" functions. These smoothing functions act essentially as low pass filters, removing small-scale power; the resulting $\sigma_0(M)$ receives contributions from power on all scales $\geq M$. The candidates for Lyα clouds reside in near-mean background environments; therefore, these density peaks receive dominant contribution from power at their mass scale. Under the application of the Gaussian or a "top-hat" filter with a filtering scale of $10^6 M_\odot$, a smoothed $10^9 M_\odot$ perturbation would register as being composed of a large number of $10^6 M_\odot$ condensates, even if the $10^9 M_\odot$ object has no structure on smaller scales. In considering only peaks resulting from power predominantly at their own mass scale (hereafter referred to as M-peaks), it is useful to define a mathematical filter designed to register on the M-peaks. Such a window function must filter the power on mass scales both larger and smaller than M, the mass of M-peaks under consideration. In § II, we introduce and discuss some of the properties of this finite band pass filter, and in § III, we use the filter to explore the formation of Lyα cloud candidates in the biased CDM model.

II. WINDOWS FOR M-PEAKS

Consider a window function $W(r; R)$ with some characteristic length scale R. A homogeneous, isotropic, Gaussian random field, $\delta(r)$, convolved with such a function yields a new Gaussian random field:

$$\Delta(r; R) = \int \delta(r')W(|\mathbf{r} - \mathbf{r}'|; R)d\mathbf{r}' , \tag{4}$$

which can be expressed more conveniently (Peebles 1980) as

$$\Delta(r; R) = \frac{1}{(2\pi)^3} \int e^{i\mathbf{k}\cdot\mathbf{r}} \delta_k \tilde{W}(k; R)d\mathbf{k} , \tag{5}$$

where $\tilde{W}(k; R)$ and δ_k are the Fourier transforms of $W(r; R)$ and $\delta(r)$, respectively.

The correlation function for $\Delta(r; R)$ is defined as

$$\xi_\Delta(|\mathbf{r} - \mathbf{r}'|) \equiv \langle \Delta(r; R)\Delta(r'; R)\rangle = \frac{1}{(2\pi)^3} \int e^{i\mathbf{k}\cdot(\mathbf{r}-\mathbf{r}')} P(k)\tilde{W}^2(k; R)d\mathbf{k} , \tag{6}$$

where $\langle \delta_{\mathbf{k}} \delta^*_{\mathbf{k}'}\rangle = P(k) \cdot \delta^3(\mathbf{k} - \mathbf{k}')$. Therefore, given the power spectrum $P(k)$ for the Gaussian field $\delta(r)$, the power spectrum for the filtered field is

$$P_\Delta(k; R) = P(k)\tilde{W}^2(k; R) . \tag{7}$$

The various moments of the filtered power spectrum are given by

$$\sigma_j^2 = \frac{1}{(2\pi)^3} \int P_\Delta(k)k^{2j} d\mathbf{k} . \tag{8}$$

The mean square fluctuation of the filtered density field σ_0^2 is equivalent to $\xi_\Delta(0)$.

For a Gaussian window function,

$$W(r; R) = \frac{1}{(2\pi)^{3/2} R^3} e^{-r^2/2R^2} , \tag{9}$$

the power spectrum of the filtered density field is

$$P_\Delta(k; R) = e^{-(kR)^2} P(k) . \tag{10}$$

The mass scale associated with the window is $M = (2\pi)^{3/2} \rho_c R^3$. In Figure 1*a*, we plot $d\sigma_0/d \log(k) (\equiv P_\Delta(k) \times k^3)$ for the biased CDM power spectrum (BBKS):

$$P_x(k) \propto [\ln(1 + 2.343\beta k)]^2 / [k(1 + 3.91\beta k + 262.1\beta^2 k^2 + 164.7\beta^3 k^3 + 2017\beta^4 k^4)^{1/2}] , \tag{11}$$

where $\beta = (\Omega h_0^2)^{-1} = 4$ (corresponding to $h_0 = 0.5$, $\Omega = 1$), and k is the comoving wavenumber in units of Mpc^{-1}, normal-

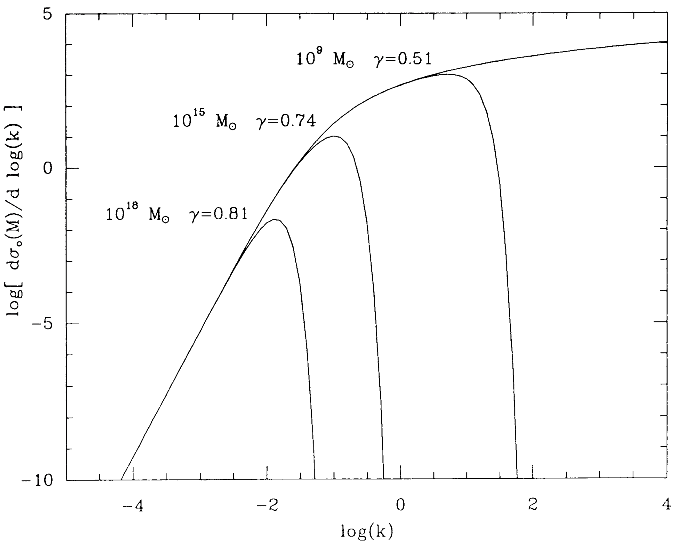

FIG. 1a

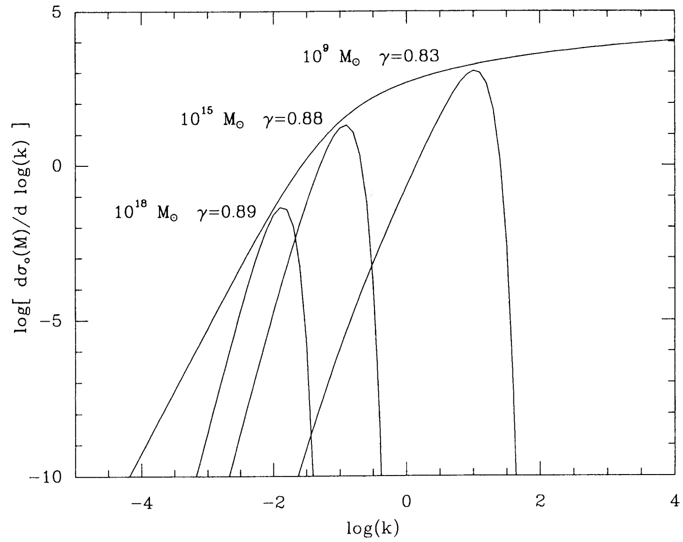

FIG. 1b

FIG. 1.—(a) Plot of $d\sigma_0/d \log(k) (\equiv P_\Delta(k) \times k^3)$ for the biased CDM power spectrum and for the Gaussian-filtered power spectrums corresponding to filtering scales 10^9, 10^{15}, and 10^{18} $M_\odot$. The parameter γ quantifies the extent of the mass range that contributes significantly to $\sigma_0(M)$. For a sharp maximum, $\gamma \approx 1$ and for a very broad maximum, $\gamma \ll 1$. For large filtering scales, $\sigma_0(M)$ receives predominant contribution from power in a small mass scale range about the scale of interest; at small filtering scales, $\sigma_0(M)$ receives significant contribution from power over a broad range of mass scales. (b) Same as (a) using the finite bandpass filter instead of a Gaussian. In contrast to the Gaussian smoothing scheme, this filter samples the power over a very limited range of mass scales at the mass scale of the "lumps" under investigation; $\gamma \approx 0.83$ for all filtering scales.

ized to the present. We also plot $d\sigma_0/d \log(k)$ for the Gaussian filtered power spectrum corresponding to filtering scales 10^9, 10^{15}, and 10^{18} $M_\odot$, and for the unfiltered power spectrum. The Gaussian filter is a low pass filter. Since $P(k) \propto k$ at large scales, $\sigma_0(M)$ results predominantly from contributions near the peak of filtered curves, which occurs at the scale of interest. For small scales, however, the Gaussian filtered curves no longer have a sharp maximum and $\sigma_0(M)$ receives significant contribution from power over a range of mass scales. The quantity $\sigma_0(M)$ cannot be identified with a structure of a well-defined mass scale. The parameter $\gamma \equiv \sigma_1^2/\sigma_2\sigma_0$ quantifies the extent of the mass range that contributes significantly to $\sigma_0(M)$. If $P_\Delta(k)$ is a delta function, $\gamma = 1$ and if $d\sigma_0/d \log(k)$ has a very broad peak, $\gamma \ll 1$ (BBKS). In Figure 1a, we show that value of the γ parameter corresponding to the different filtering scales; γ decreases as M decreases and the associated curve develops an increasingly broader maximum.

In order to study M-peaks of a given mass scale $M \ll 10^{15}$ $M_\odot$, we need to define a filter that minimizes the effects of larger background density perturbations. The required window function must ignore the mean and the gradients in a density field that it is convolved with

$$\int (A + \boldsymbol{B} \cdot \boldsymbol{x}) W(\boldsymbol{r} - \boldsymbol{x}) d\boldsymbol{x} = 0 \quad (12)$$

for all finite A, $\boldsymbol{B}$; it should only notice "lumps" of some mass scale related to the scale of the window. An appropriately normalized second derivative of a Gaussian has the desired properties

$$W(r; R) = \frac{3}{4\pi R^3}\left(\frac{e}{3}\right)^{3/2}\left[1 - \frac{1}{3}\left(\frac{r}{R}\right)^2\right] e^{-r^2/2R^2} . \quad (13)$$

This window has a positive central peak ($0 \le r \le \sqrt{3}\,R$) of unit volume and a negative lobe of equal volume for $r \ge \sqrt{3}\,R$. The window, therefore, selectively picks out "lumps" of mass scales corresponding to the scale of the positive central region,

$$M = \frac{4\pi}{3}\rho_c R^3 \left(\frac{3}{e}\right)^{3/2} . \quad (14)$$

The power spectrum of the filtered density field is

$$P_\Delta(k; R) = \frac{\pi}{2}\left(\frac{e}{3}\right)^3 (kR)^4 e^{-(kR)^2} P(k) . \quad (15)$$

The window function, as shown in Figure 1b, is a finite bandpass filter. In contrast to the Gaussian smoothing scheme, this filter samples the power over a very limited range of wavenumbers corresponding to the mass scale of the "lumps" under investigation; the breadth of the maximum is only weakly dependent of the filtering mass scale. The value of the γ parameter is essentially constant: $\gamma \approx 0.83$. This is just the kind of filter we need to study the M-peaks. After all, the M-peaks are "lumps" of a given mass scale. By removing the large-scale power, the filter yields the height of an M-peak relative to the local background density, i.e., $\bar{\rho}\Delta$ is essentially the density enhancement in the M-peak relative to the local background; $\bar{\rho}$ is the global mean density. For an M-peak in a near-mean environment, the filter yields the actual density fluctuation of the peak. We shall henceforth refer to the new window function as a "matched filter."

In Figures 2a and 2b, we show the matched window (*solid curve*) and the Gaussian window (*dashed curve*) in $\boldsymbol{r}$-space. For a given filtering mass scale, the ratio of the Gaussian filtering scale to that for the matched filter is $R_g/R_m \approx 0.68$. In Figure 2c, we show the two filters in Fourier space. The Gaussian window is a low bandpass filter; it squelches power on mass scales smaller than the filtering scale. The matched filter, on the other hand, is a finite bandpass filter with a FWHM extending from $\sim\frac{1}{3}M$ to $\sim 3M$ where M is the filtering mass scale.

In order to illustrate the function of the matched filter, we simulated a two-dimensional Gaussian random field on a

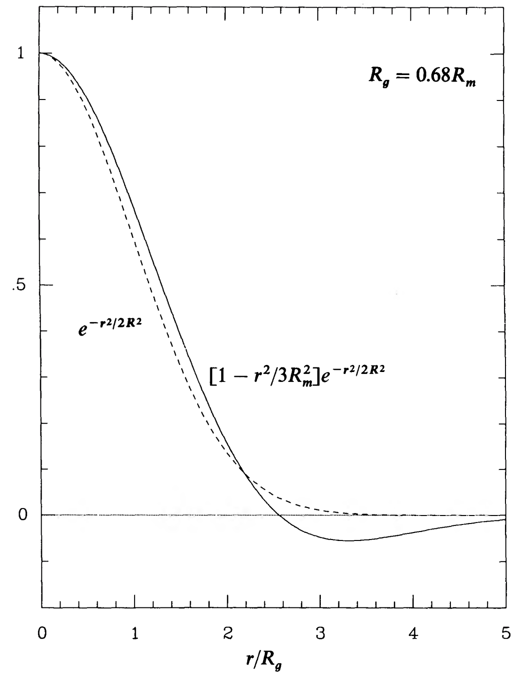

FIG. 2a

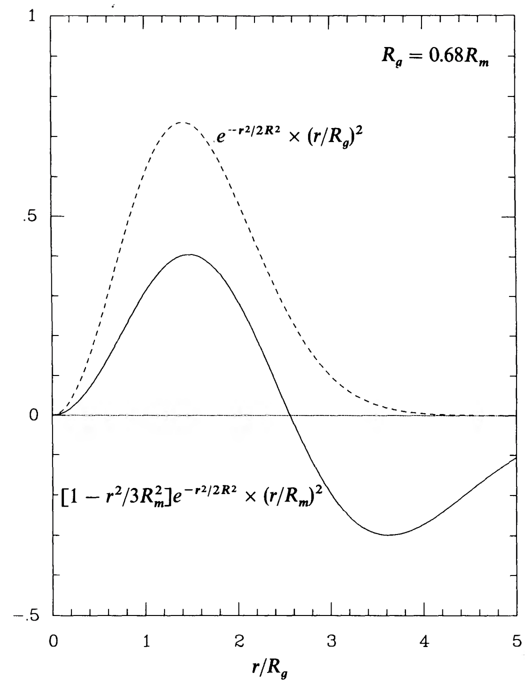

FIG. 2b

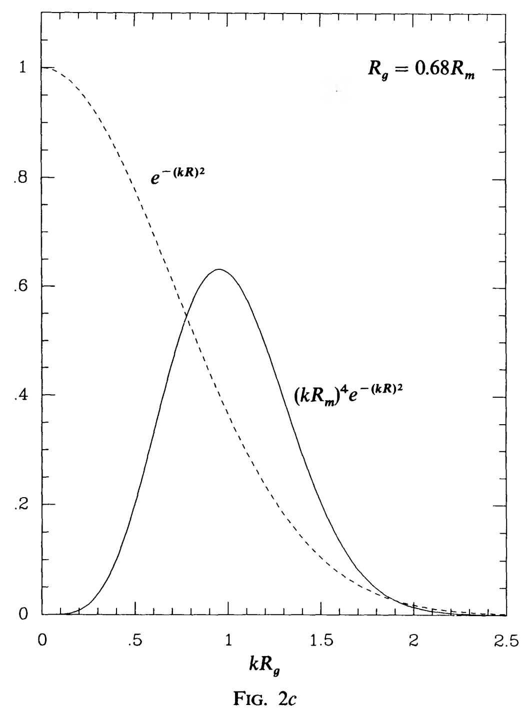

FIG. 2c

FIG. 2.—(a) The matched window (*solid curve*) and the Gaussian window (*dashed curve*) in r-space. The matched window has a positive central peak ($0 \leq r \leq \sqrt{3}\,R_m$) of unit volume and a negative lobe of equal volume for $r \geq \sqrt{3}\,R_m$. It therefore selectively picks out "lumps" of mass scales corresponding to the scale of the positive central region. For a given filtering mass scale, the ratio of the Gaussian filtering scale to that for the march filter is $R_g/R_m \approx 0.68$. (b) Same as in (a) except the window functions are weighted by r^2 term appearing in the volume integrals. The plot graphically shows the positive and the negative equal volume lobes of the matched filter. (c) The matched filter and the Gaussian filter in Fourier space. The Gaussian window is a low bandpass filter and as a result, only squelches power on mass scales smaller than the filtering scale. The matched filter, on the other hand, is a finite bandpass filter with a FWHM extending from $\sim\frac{1}{3}M$ to $\sim 3M$ where M is the filtering mass scale.

periodic square of area 100 Mpc^2, with a power spectrum having the same form as that for CDM with adiabatic initial fluctuations (cf. eq. [11]). We filtered the Gaussian random field with the Gaussian filter and with the matched filter:

$$W(kR_g) = e^{-(kR_g)^2/2}\,, \qquad A = 2\pi R_g^2\,;$$
$$W(kR_m) = \left(\frac{e}{2}\right)(kR_m)^2\, e^{-(kR_m)^2/2}\,, \quad A = \frac{2\pi}{e}\, R_m^2\,; \tag{16}$$

where A is the area corresponding to the filtering scale. We chose $A = \pi/50$ Mpc^2 as we are particularly interested in small-scale structure. The contour map of the Gaussian-filtered realization is shown in Figure 3a. The distance between the adjacent tick marks delineates the filtering length scale. The solid contours correspond to $n\sigma$ levels $n = 0.5, 1.0, \ldots, 3.0$, where $\sigma = 69.8$, the rms fluctuation for the Gaussian filtered field; the dotted contours are the corresponding negative sigma level. Since the Gaussian filter only removes power on scales smaller than the filtering length, the positive density regions in the map are in general much larger than the filtering scale. In Figure 3b, we show the contour map of the same density field realization but filtered by a matched filter. The contour levels have the same values as in Figure 3a. The matched filter performs as expected. It selects out structures comparable in scale to the filtering area (M-peaks in two-dimensions) while fluctuations larger than the filtering scale are removed. A comparison of the two contour plots reveals that the matched filter, however, does not discriminate between the different embedding environments of the small-scale structure; not all of the peaks in Figure 3b are isolated "lumps." We shall address this issue later in the paper.

The epoch of formation of structures with mass M is generally taken to be the epoch at which the mass scale enters non-linear growth phase: $\sigma_0(M) \sim 1$. In order to estimate the epoch of formation of isolated small-scale M-peaks in the biased CDM model, the appropriate $\sigma_0(M)$ is that calculated using the matched filter. We consider the biased standard CDM

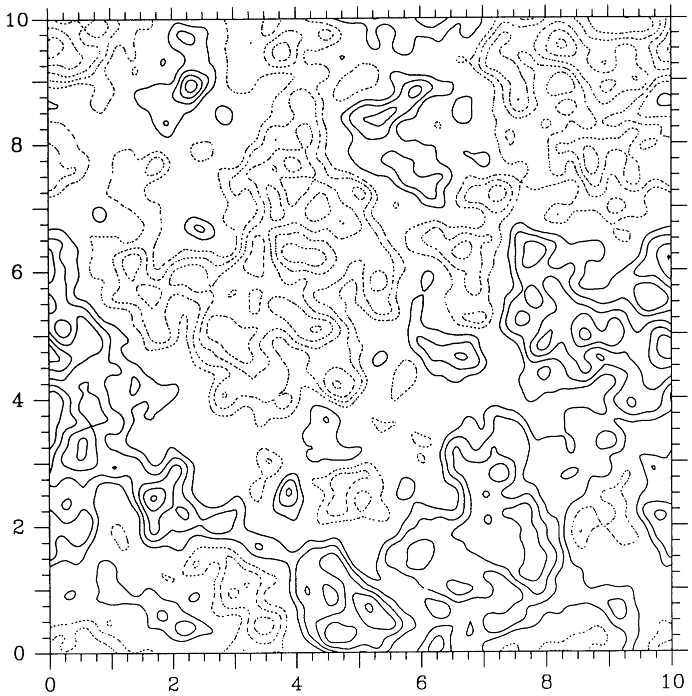

FIG. 3a

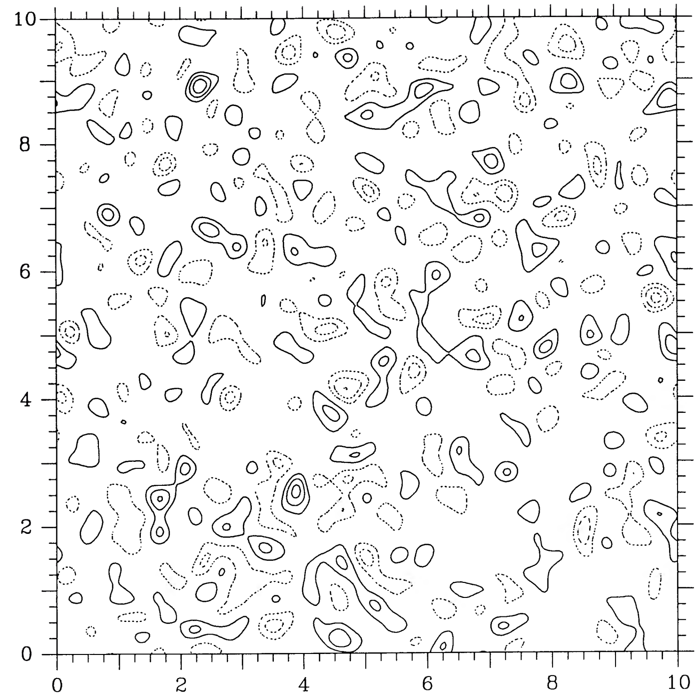

FIG. 3b

FIG. 3.—(*a*) A contour map of the Gaussian-filtered realization of a two-dimensional Gaussian random field with the power spectrum having the same form as that for CDM with adiabatic initial fluctuations. The area corresponding to the filtering scale is $A = \pi/50$ Mpc^2 and the distance between adjacent tick marks delineates the filtering length. The solid contours correspond to $n\sigma$ levels $n = 0.5, 1.0, \ldots, 3.0$, where $\sigma = 69.8$, the rms fluctuation for the Gaussian-filtered field; the dotted contours are the corresponding negative sigma level regions. Since the Gaussian filter only removes power on scales smaller than the filtering length, the positive density regions in the map are in general much larger than the area of filtering. (*b*) A contour map of the same realization shown in (*a*) acted upon by the matched filter. The contour levels have the same values as in (*a*). The matched filter selects out structures comparable in scale to the filtering area (equivalent of M-peaks) while fluctuations larger than the filtering scale are removed.

model with $\Omega = 1$, $\Omega_b = 0.1$, $h_0 = 0.5$. The power spectrum (cf. eq. [11]) is normalized such that the rms density fluctuation evaluated using a "top-hat" filter corresponds to $\sigma_0 = 1/2.6$ at $R = 8h^{-1}$ Mpc at present (Davis *et al.* 1985). In Figure 4, we plot the height of a 1 σ density fluctuation at redshift $z = 2.5$ calculated using the matched filter (*solid curve*) and the Gaussian filter (*dashed curve*). On large scales, due to the form of the CDM power spectrum, $\sigma_0(M)$ results predominantly from fluctuations on scale M. Therefore, both the Gaussian and the matched filters perform alike. The slight difference is due to the Gaussian window's mild filtering of power on the scale of interest. On the small scales, the removal of background fluctuations leads to a significant difference between the rms density fluctuations calculated using the two filtering schemes. In particular, at redshift $z = 2.5$, the Gaussian window suggests that the bulk of the density peaks of scale $M \sim 10^{10} M_\odot$ are entering nonlinear growth phase while the matched filter shows that this is certainly not true of the $10^{10} M_\odot$ M-peaks in near-mean background; typical isolated objects of this mass scale cannot be considered to have been formed by $z = 2.5$

In order to further verify that the matched filter performs as described, we consider the following exercise: Given a Gaussian smoothed density $\Delta_g(\boldsymbol{x}, M)$ [hereafter, $\Delta_g(\boldsymbol{x})$], we wish to calculate the 1 σ peak heights of density fluctuations of mass scale M. We expect that for such peaks, the angle-averaged density fluctuation on the surface of a sphere of mass scale $\sim M$ centered on the peak is small. We denote the angle-

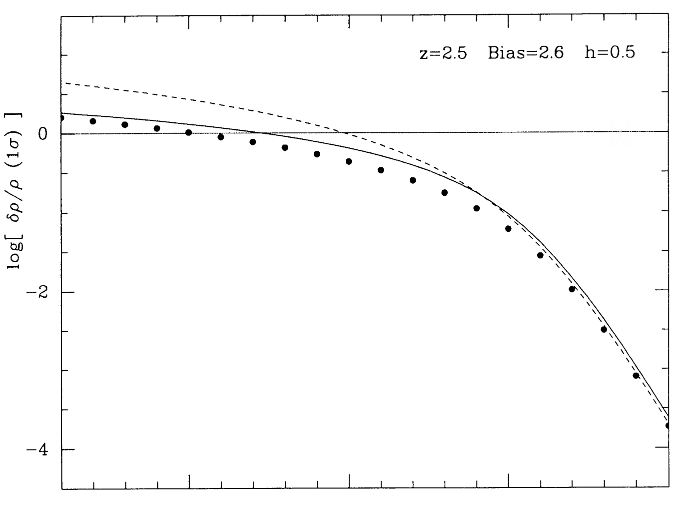

FIG. 4.—1 σ level of density fluctuations at redshift $z = 2.5$, calculated using the matched filter (*solid curve*) and the Gaussian filter (*dashed curve*). At small mass scales, the removal of background fluctuations by the matched filter leads to a significant difference between the rms density fluctuations calculated using the two filtering schemes. For further comparison, we also plot the 1 σ height of "isolated" density fluctuations in the Gaussian-filtered scheme (*filled dots*). The loci of these points agree surprisingly well with the 1 σ level determined using the matched filter.

averaged density fluctuation on the surface of a sphere of mass scale M located at $\boldsymbol{x}$, as

$$\bar{\Delta}_g(\boldsymbol{x}; r) = \int \Delta_g(\boldsymbol{x}') \cdot \frac{\delta[|\boldsymbol{x} - \boldsymbol{x}'| - r]}{4\pi r^2} \, d\boldsymbol{x}' , \qquad (17)$$

where r is the radius of the sphere. Note that $\Delta_g(\boldsymbol{x}) \equiv \bar{\Delta}_g(\boldsymbol{x}; 0)$.

Both $\Delta_g(\boldsymbol{x})$ and $\bar{\Delta}_g(\boldsymbol{x}; r)$ are Gaussian random variables. Given a set of Gaussian random variables $\boldsymbol{y} = (y_1, y_2, \ldots, y_n)$, the joint probability distribution is

$$P(\boldsymbol{y})d\boldsymbol{y} = \frac{\exp\left(-\frac{1}{2}\sum \xi_{ij}^{-1} y_i y_j\right)}{[(2\pi)^n \det(\xi)]^{1/2}} \, d\boldsymbol{y} , \qquad (18)$$

where the covariance matrix $\xi_{ij} = \langle y_i y_j \rangle$; we have assumed that $\langle y_i \rangle = 0$. Therefore, the joint probability distribution for the density fluctuation at a given point $\Delta_g(\boldsymbol{x})$ and $\bar{\Delta}_g(\boldsymbol{x}; r)$, the angle-averaged density fluctuation at a distance r about the same point, is

$$P(v, \bar{v}_r)dv\, d\bar{v}_r = \frac{1}{2\pi} \frac{1}{\sqrt{\phi - \psi^2}} \times \exp\left\{ -\frac{1}{2}\left[v^2 + \frac{(\bar{v}_r - \psi v)^2}{\phi - \psi^2} \right] \right\} dv\, d\bar{v}_r , \qquad (19a)$$

where

$$\psi = \frac{\langle \Delta_g(0)\, \Delta_g(r) \rangle}{\langle \Delta_g^2 \rangle} \quad \text{and} \quad \phi = \frac{\langle \bar{\Delta}_g^2(r) \rangle}{\langle \Delta_g^2 \rangle} . \qquad (19b)$$

We have expressed the density fluctuations in terms of the rms fluctuation of the Gaussian smoothed field: $v \equiv \Delta_g(\boldsymbol{x})/\sigma_{0g}$ and $\bar{v}_r \equiv \bar{\Delta}_g(\boldsymbol{x}; r)/\sigma_{0g}$. Designating a density fluctuation $\Delta_g(\boldsymbol{x})$ as "isolated" if $-0.5 \le \bar{v}_r \le 0.5$, we evaluated the mean and the variance of such fluctuations. For all practical purposes, the mean is negligible with respect to the rms. In Figure 4, we plot the corresponding 1 σ height of "isolated" density fluctuations (*filled dots*). The loci of these points agree surprisingly well with the 1 σ level determined using the matched filter.

Apart from calculating the rms density fluctuations associated with isolated M-peaks, we are also interested in determining the number density (comoving) of such structures. The "matched filtered" field is a three-dimensional Gaussian random field; therefore, the differential number density of M-peaks is well approximated by

$$\mathcal{N}_{\rm Mpk}(v) = \frac{1}{(2\pi)^2 R_*^3} \, G(\gamma, v\gamma)\, e^{-v^2/2} , \qquad (20)$$

where a fitting formula for $G(\gamma, v\gamma)$ is given in equation (4.4) of BBKS. As defined earlier, the parameter v measures the height of the density peak: $v = \Delta/\sigma_0$ and $\gamma = \sigma_1^2/\sigma_2 \sigma_0$ while $R_* = \sqrt{3}\,\sigma_1/\sigma_2$; σ_j are the various moments of the power spectrum.

In Figure 5, we plot the comoving number density of M-peaks (*solid line*) whose peak heights are at or above some threshold level with respect to the local background. For comparison, we also show the comoving number density of peaks for Gaussian filtered field (*dashed line*). In the Gaussian filtered scheme, the global mean density is the zero-point for the peaks heights and the corresponding threshold levels. For a proper comparison, we are required to choose some specific threshold level for the peak heights; we cannot simply set a threshold for v because v measures the peaks heights relative to the rms fluctuation of the density field and the values of the rms fluctuation differ for the filtering schemes. We plot results for four different threshold levels (we have expressed the peak threshold heights in terms of the rms fluctuation for the Gaussian filtered field).

For low threshold levels, the number density of peaks for the two filtering schemes are identical. In the Gaussian scheme, the number density of peaks includes all peaks of mass scale greater than the filtering scale. For the matched filtered field, only peaks of mass scale comparable to the filtering scale are counted. It would appear that there ought to be more peaks in the Gaussian filtered density field. However, peaks (particularly M-peaks), which are depressed below the threshold level due to modulations by larger fluctuations in the Gaussian scheme, are brought to the fore by the matched filter and thereby counted. The matched filter removes power on scales larger as well as smaller than the filtering scale.

For high threshold levels and low mass scales, the number density of peaks whose height above the local background (intrinsic height) exceeds the threshold level is smaller than the number density of peaks with total height greater than the threshold. This is expected. The CDM power spectrum exhibits decreasing power on small scales, which in turn leads to intrinsically small peak heights. However, the background power plays an important role of lifting the small scale peaks, resulting in large total heights.

At this point, we distinguish between M-peaks in general and isolated M-peaks. Isolated peaks are those which reside in near-mean environments. A "lump" of mass M atop some larger positive density fluctuation would not be classified as being isolated; it would, however, be classified as an M-peak and would be found by the matched filter. The matched filter removes the large-scale power and hence, the resulting M-peaks essentially retain their intrinsic height (height relative to the local background density level). For the purposes of calculating the rms density fluctuation for peaks of a given mass scale in near-mean background, it does not matter whether we particularly focus on actual isolated M-peaks or whether we use the matched filter to remove the large background fluctuations and treat all the M-peaks as "isolated." We are simply interested in determining the rms intrinsic height which, for isolated M-peaks, is the actual rms density fluctuation.

On the other hand, in order to determine the number density of true isolated M-peaks, we need to consider the background density fluctuations so that the peaks in near-mean background can be distinguished from the peaks that are part of some larger structure but simply appear as isolated upon the application of the matched filter. We shall address this issue in the next section, in the specific context of isolated $\sim 10^9\, M_\odot$ objects, the candidates for Lyα clouds.

III. Lyα CLOUD CANDIDATES

In § I, we noted that in a CDM cosmogony the Lyα cloud candidates are most likely low-mass ($\sim 10^9\, M_\odot$) density peaks in near-mean environments, or in terms of the terminology introduced in this paper, Lyα cloud candidates are most likely isolated M-peaks. To determine whether an M-peak is isolated or not, we need to probe its background density field. We measure the background density by smoothing the unfiltered density field with a Gaussian of filtering scale larger than the mass scale of the M-peaks. We shall denote the background field by $v_b(\boldsymbol{r}) \equiv \Delta_b(\boldsymbol{r})/\sigma_{0b}$ where $\sigma_{0b} \equiv \sigma_{0g}(M_b)$, and the density field of M-peaks by $v_m(\boldsymbol{r}) \equiv \Delta_m(\boldsymbol{r})/\sigma_{0m}$.

We classify a given M-peak density fluctuation $v_m(\boldsymbol{r})$ as "isolated" if the background density fluctuation at the same

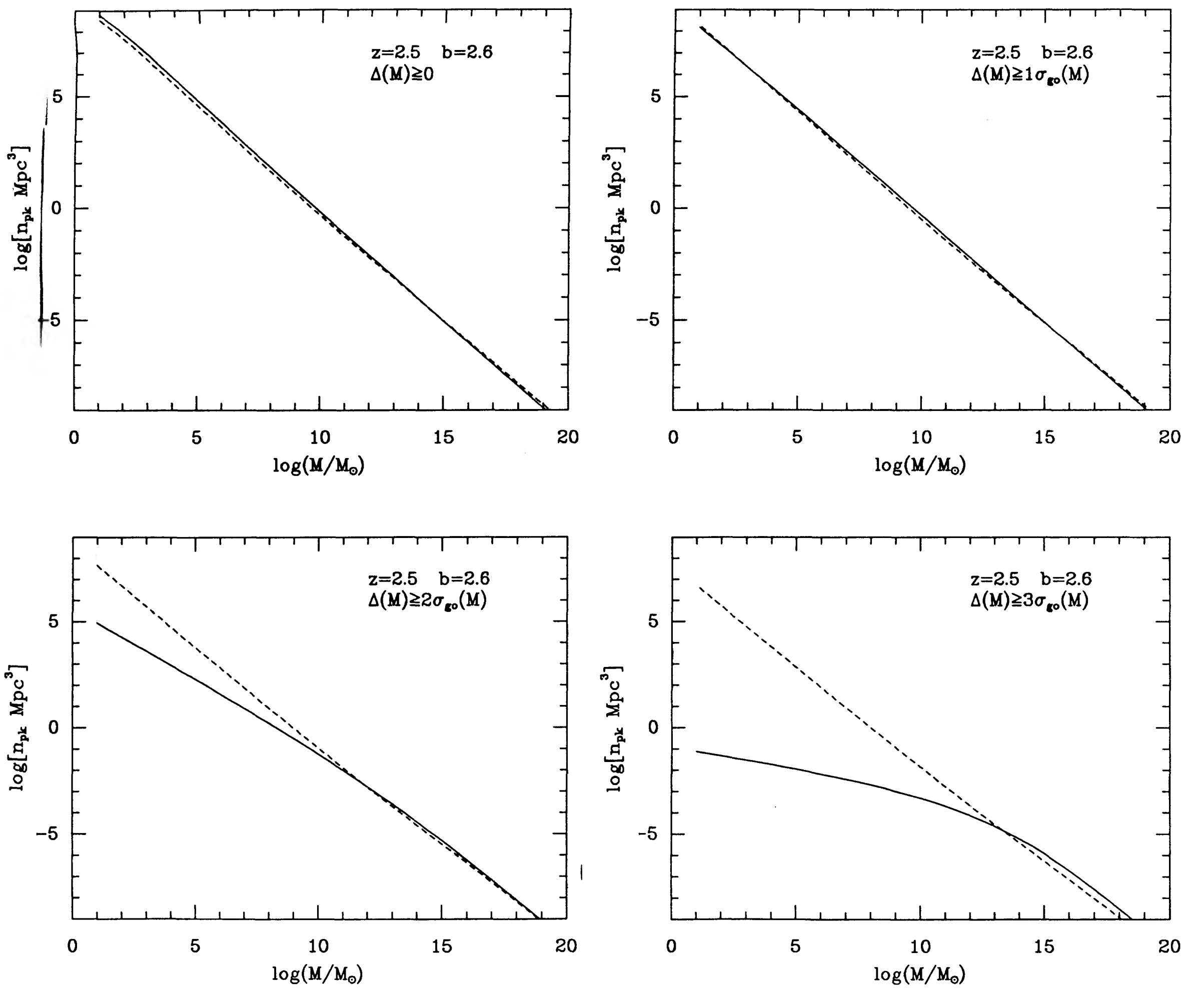

FIG. 5.—The comoving number density of M-peaks (*solid line*) whose peak heights are some threshold level above the local background. For comparison, we also show the comoving number density of peaks for Gaussian-filtered field (*dashed line*). In the Gaussian-filtered scheme, the global mean density is the zero point for the peaks heights and the threshold levels. We plot results for four different threshold levels (the peak threshold heights are expressed in terms of the rms fluctuation for the Gaussian-filtered field).

location is small: $-0.5 \le \nu_b(\boldsymbol{r}) \le 0.5$. The resulting differential number density of isolated M-peaks is

$$\mathcal{N}_{\rm ipk}(\nu_m) = \mathcal{N}_{\rm Mpk}(\nu_m) \int_{-0.5}^{0.5} P(\nu_b \,|\, \nu_m) d\nu_b \,. \tag{21}$$

The conditional probability is given by

$$P(\nu_b \,|\, \nu_m) d\nu_b = \frac{P(\nu_b, \nu_m)}{P(\nu_m)} d\nu_b \,, \tag{22}$$

where $P(\nu_b, \nu_m) d\nu_b d\nu_m$ is the joint probability condition (cf. eq. [18]). Therefore,

$$P(\nu_b \,|\, \nu_m) = \frac{1}{\sqrt{2\pi(1-\chi^2)}} \exp\left\{-\frac{1}{2}\frac{(\nu_b - \chi\nu_m)^2}{1-\chi^2}\right\} \tag{23a}$$

and

$$\chi^2 = \frac{\langle \Delta_b(0)\Delta_m(0)\rangle^2}{\langle \Delta_b^2\rangle\langle \Delta_m^2\rangle} \,. \tag{23b}$$

In the specific case of Lyα cloud candidates, we are interested in M-peaks of scale $M \sim 10^9\ M_\odot$ and we choose to smooth the background at $M_b \sim 10^{11}\ M_\odot$, a galactic mass scale. In essence, we shall ignore M-peaks superposed on fluctuations of mass scale $M \ge 10^{11}\ M_\odot$. The corresponding cross-correlation between the two density field is quite small: $\chi \approx 0.1$; increasing the background smoothing scale results in even smaller values for χ. The number density of candidate peaks for Lyα clouds is

$$n_{\rm Ly\alpha} = \int_{\nu_t}^{\infty} \mathcal{N}_{\rm ipk}(\nu_m) d\nu_m \,. \tag{24}$$

For threshold level ν_t ranging from 0 to 4, the isolation condition "$-0.5 \le \nu_b \le 0.5$" only reduces the number of peaks by a factor of 3–4. The peak threshold density for the cloud candidates is determined by requiring the neutral hydrogen column density to be $N_{\rm H\,I} \ge 10^{14}$ cm^{-2} at the epoch of observation, which we shall take as $z = 2.5$.

Within the framework of Rees's (1986) model for the Lyα clouds, in order to gravitationally confine isothermal gas of $T \sim 3 \times 10^4$ K within structures of radii $R_{\rm cl} \sim 10$ kpc, the total mass of the structure must be $M \sim 10^{9.5}\ M_\odot$ from the virial theorem. The CDM collapse, assuming a spherical collapse model (Peebles 1980) with virialization at half the turn-around radius, ensues according to

$$\left(\frac{R_{\rm CDM}}{10\ \rm kpc}\right) \sim \begin{cases} \dfrac{2.82}{1+z}\, h_0^{-2/3} \left(\dfrac{M}{10^9\ M_\odot}\right)^{1/3} \dfrac{1-\cos\theta}{\Delta(M, z)}\,, & \text{if } 0 \le \theta \le 2\pi\,; \\ \dfrac{2.82}{1+z}\, h_0^{-2/3} \left(\dfrac{M}{10^9\ M_\odot}\right)^{1/3} \dfrac{1}{\Delta(M, z)}\,, & \text{after virialization.} \end{cases} \tag{25}$$

In the above equation, $\Delta(M, z)$ is the linearly extrapolated overdensity of the condensate at redshift z: $\Delta(M, z) = \Delta_0(t/t_0)^{2/3}$; i.e., $\Delta(M, z) \approx 0.495(\theta - \sin\theta)^{2/3}$, if $0 \le \theta \le 2\pi$.

The gas collapse follows the CDM collapse until pressure support becomes important. We assume that at this time the cloud of radius $R_{\rm cl} \approx R_{\rm CDM}$ has formed, regardless of the continuing collapse and the subsequent virialization of the dark matter. For $R_{\rm cl} \approx 10$ kpc and $M \sim 10^{9.5}\ M_\odot$ at $z = 2.5$, we find that required linearly extrapolated overdensity is $\Delta \gtrsim 1.62$. Therefore, if Lyα absorption lines are due to stably confined gas in dark "minihalos," the required structures correspond to 2.4 σ_{0m} peaks where $\sigma_{0m} \approx 0.68$ is the rms density fluctuation for isolated $10^{9.5}\ M_\odot$ M-peaks at $z = 2.5$. The comoving number density of candidate objects is $n_{\rm Ly\alpha} \approx 10^{-2.2}$ Mpc^{-3}.

If Lyα clouds are *dynamical* entities as proposed by BSS, the appropriate structures span the mass range 10^9–$10^{10}\ M_\odot$. The distribution of gas in these low-mass condensates cannot be easily estimated. The interplay between the pressure-driven expansion of the photoionized gas and the gravitational contraction due to the pull of the collapsing CDM is quite complicated and therefore, the nonlinear evolution of the density in the clouds is best studied by numerical simulations. Based on the results of numerical simulations presented by BSS, for spherically symmetric, isolated clouds with $N_{\rm H\,I} \gtrsim 10^{14}$ cm^{-2} at $z = 2.5$, the peak threshold is $\nu_t \approx 2.4$ (in units of σ_{0m}) for $10^{9.5}\ M_\odot$ in a CDM model with biasing factor of $b = 2.6$, increasing rapidly as mass scale of the density peaks decreases. The comoving number density of cloud candidates is, therefore, not too different from that estimated for the previous model.

Having estimated the comoving number density of cloud candidates, we can determine the number of Lyα lines expected to be seen at redshift $z = 2.5$ along a given line of sight. The distribution of the clouds in redshift along a line of sight is (Sargent *et al.* 1980)

$$f(z)dz = n_{\rm Ly\alpha}(z) \times (1+z)^3 \times (\pi R_{\rm cl}^2) \times dl\,. \tag{26}$$

The path length-redshift relationship for $\Omega = 1$ universe is

$$dl = \frac{c}{H_0}(1+z)^{-5/2}dz = 3000h_0^{-1}(1+z)^{-5/2}dz\ \text{Mpc}\,. \tag{27}$$

Hence,

$$f(2.5) \approx 2h_0^{-1}n_{\rm Ly\alpha}(2.5)\left(\frac{R_{\rm cl}}{10\ \rm kpc}\right)^2 \approx 0.012h_0^{-1}\left(\frac{R_{\rm cl}}{10\ \rm kpc}\right)^2\,. \tag{28}$$

According to the observations, $f_{\rm obs}(2.5) \approx 60$. Therefore, if Ly$\alpha$ cloud candidates are indeed associated with density peaks in near-mean background, then at redshift $z = 2.5$ the comoving number density of Lyα cloud candidates in an $\Omega = 1$, $h_0 = 0.5$ CDM model with biasing factor of $b = 2.6$ is approximately three orders of magnitude too small to account for the observed number of Lyα lines.

Rescaling the above results for biasing factor of $b = 1.7$, the biasing factor adopted by BSS, we find that threshold density for Lyα cloud candidates is $\Delta_t \approx 1.6\ \sigma_{0m}$ for $M \sim 10^{9.5}\ M_\odot$ condensates. The number density of isolated M-peaks satisfying the threshold condition is $n_{\rm Ly\alpha} \approx 10^{-0.8}$ Mpc^{-3}. Even for such an optimistic biasing factor, the number density of candidate objects is two orders of magnitude too small.

The above results are not surprising. Even with the use of a Gaussian filter, the comoving number density of peaks at mass scale M is $n_{\rm pk}(\nu \ge 1, M) \approx 4.8h_0(M/10^9\ M_\odot)^{-1}$ Mpc^{-3} (BSS), adopting an extremely optimistic peak threshold level. This number density includes all peaks of mass scale M of total height greater than or equal to the value of the rms fluctuation, regardless of their local background environment as well as peaks of larger mass scales. At $z = 2.5$, the number of peaks per unit redshift along a line of sight is $f(2.5) \approx 9.6(M/10^9\ M_\odot)^{-1}(R_{\rm cl}/10\ \rm kpc)^2$, which is marginal at best. The comoving number density of Lyα cloud candidates, isolated peaks of appropriate mass scales, is expected to be even smaller.

The Lyα clouds, if they have their origins in the primordial density fluctuations as suggested by Rees (1986) and BSS, can be used to probe the amplitude of the power spectrum on subgalactic scales. Assuming that the Lyα absorption lines are due to weakly correlated cosmological distribution of distinct, isolated low-mass condensates, the analysis presented in this paper suggests that the CDM power spectrum, even with an optimistic normalization, does not have sufficient power on subgalactic scales to account for the observed structures.

The author is indebted to J. P. Ostriker for suggesting this investigation and for guidance during the course of the study. The author would also like to acknowledge R. Juszkiewicz, J. E. Gunn, P. J. E. Peebles, S. White, D. H. Weinberg, and N. Katz for helpful criticisms and suggestions. A. B. is supported by a NSERC (Canada) postgraduate fellowship. This work was supported by NASA grant NAGW-756 to Princeton University.

REFERENCES

Bajtlik, S., Duncan, R. C., and Ostriker, J. P. 1988, *Ap. J.*, **327**, 570.
Bardeen, J. M., Bond, J. R., Kaiser, N., and Szalay, A. S. 1986, *Ap. J.*, **304**, 15 (BBKS).
Bond, J. R., Szalay, A. S., and Silk, J. 1988, *Ap. J.*, **324**, 627 (BBS).
Davis, M., Efstathiou, G., Frenk, C. S., and White, S. D. M. 1985, *Ap. J.*, **292**, 371.
Foltz, C. B., Weymann, R. J., Rosen, H.-J., and Chaffee, F. H. 1984, *Ap. J. (Letters)*, **281**, L1.
Gunn, J. E., and Peterson, B. A. 1965, *Ap. J.*, **142**, 1633 (GP).
Huchra, J., Geller, M., de Lapparent, V., and Burg, R. 1987, in *IAU Symposium 130, Evolution of Large Scale Structures in the Universe*, ed. J. Audouze, M-C. Pelletan, and A. Szalay (Dordrecht: Reidel), p. 105.
Ikeuchi, S., and Ostriker, J. P. 1986, *Ap. J.*, **301**, 522.
Oort, J. H. 1981, *Astr. Ap.*, **94**, 359.
Ostriker, J. P. 1987, in *QSO Absorption Lines: Probing the Universe*, ed. J. C. Blades, D. A. Turnshek, and C. A. Norman (Cambridge: Cambridge University Press).
Ostriker, J. P., Bajtlik, S., and Duncan, R. C. 1988, *Ap. J. (Letters)*, **327**, L35.
Ostriker, J. P., and Strassler, M. 1989, *Ap. J.*, **338**, 579.
Peebles, P. J. E. 1980, *The Large Scale Structure of the Universe* (Princeton: Princeton University Press).
Rees, M. J. 1986, *M.N.R.A.S.*, **218**, 25P.
Sargent, W. L. W., Young, P. J. Boksenberg, A., and Tyler, D. 1980, *Ap. J. Suppl.*, **42**, 41.
Steidel, C. C., and Sargent, W. L. W. 1987, *Ap. J. (Letters)*, **318**, L11.
Webb, J. K. 1987, in *IAU Symposium 124, Observational Cosmology*, ed. A. Hewitt, G. Burbidge, and Li-Zhi Fang (Dordrecht: Reidel), p. 803.

ARIF BABUL: Institute of Astronomy, Madingley Rd., Cambridge, CB3 0HA, England